FRESH IMPACT CRATER DETECTION FROM DIFFERENCE MAPPING OF CTX IMAGES. J. W. Sneed[1]*, M. D. Day[1], and K. S. Edgett[2], [1]University of California at Los Angeles, Los Angeles, CA (*sneedjw@g.ucla.edu), [2]Malin Space Science Systems Inc., San Diego, CA.

Introduction: The martian surface records diverse and ongoing processes, including eolian dust transport and deposition, eolian dune migration, sublimation, mass wasting, and impact cratering [1-3]. Impact craters in particular provide important information about the surface exposure ages [4], subsurface geology [5], and planetary obliquity [6]. The flux of impacts to Mars has decreased over the history of the planet [7], but new impacts still occur on Mars today [8]. More than 400 recent impacts have been identified in CTX images and confirmed via HiRISE imaging [9]; these are found through human observation of changes between time-separated images (Fig. 1ab) [10]. However, these detections rely on dust redistribution in the target area, with a known bias towards heavily dust-mantled regions including Amazonis, Tharsis, and Arabia. Accordingly, previous identifications of recent impacts capture only a sample of the total set of modern martian impacts. The modern impact rate may soon be constrained by surface observation conducted by the InSight lander's SEIS (Seismic Experiment for Interior Structure) instrument [11]. Expected to catalogue impacts throughout its two-year primary mission, SEIS will provide a new experimental perspective on modern impacts to Mars. In this work, we present a third method for detecting modern impacts that will complement experimental and human-eye-based methods.

At the present time, CTX coverage exceeds 99.6% of the martian surface [12]. Overlap between CTX images is common, with >65% of the surface covered by two or more images. Among the ~100,000 CTX images collected as of October 2018 there exist 1.4 million unique pairs of CTX images with overlapping coverage of at least 1 km^2. Collectively, these overlapping regions form a considerable volume of data where the pre- and post-impact surfaces from a recent impact might have been imaged. To overcome the practical challenges of a human survey of such a large dataset, we have developed an automated tool for new crater

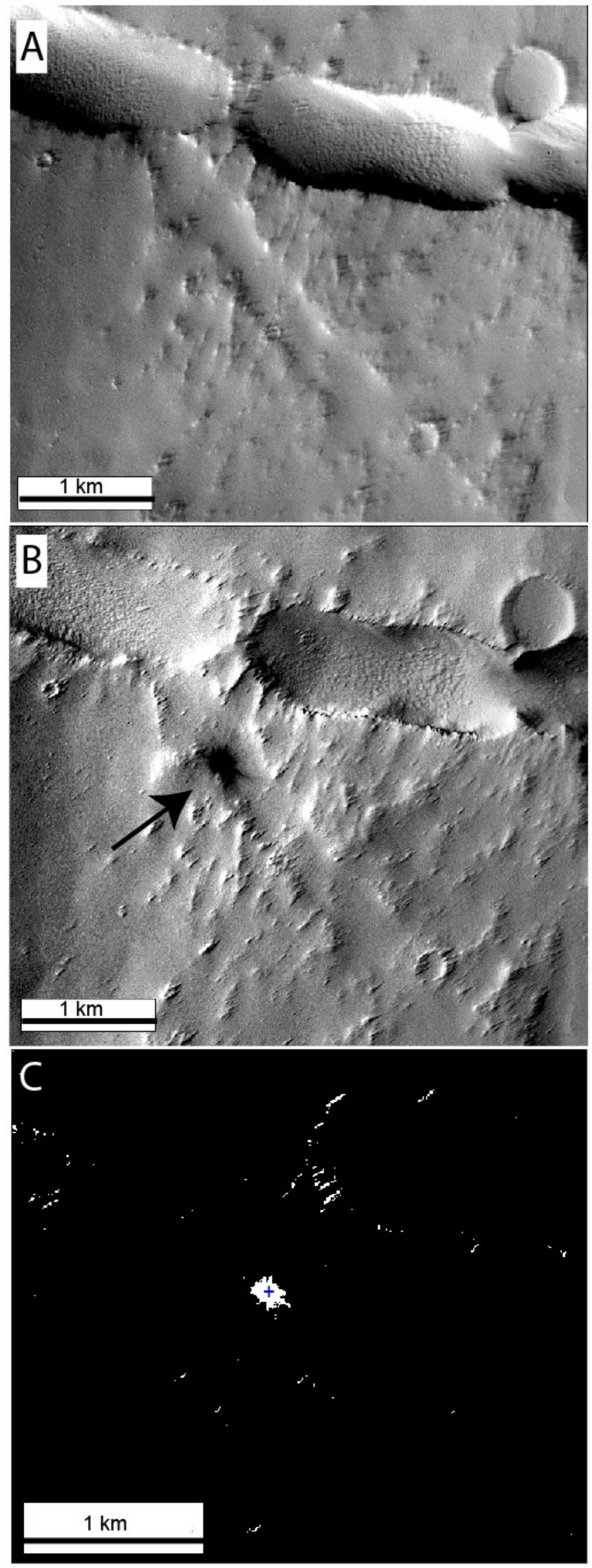

Fig 1: Fresh impact crater site catalogued by [9]. **A)** Pre-impact CTX image B09_013193_1810_XI_01N111W. **B)** Post-impact CTX image G18_025087_1836_XI_03N111W, fresh crater indicated by arrow. **C)** Successful impact detection (blue cross) in aligned binary difference map. Note secondary pixel groups (white) associated with shadows, which must be distinguished from new craters.

detection in overlapping CTX coverage, scalable in principle to all 1.4 million CTX image pairs. Initial application of this system will be limited to a longitudinal arc from -5° to 25°, chosen for its representative topography.

Detecting fresh craters: Our automated process for identifying new craters is composed of four main stages: pairwise cropping, image alignment, difference mapping, and filtering for fresh impacts.

First, each pair of overlapping images is loaded in ArcGIS and cropped to a polygon defining the overlapping section of the image. Where three or more CTX image pairs all overlap the same area, it is possible in principle to include only the earliest and latest image of each set; however, we test all possible pairings for completeness.

Due to minor variations in georeferencing, as well as inconsistencies between images (e.g., spacecraft orientation, incidence angle, and image contrast), direct pixel-to-pixel comparisons between CTX images do not reflect actual changes in the landscape. We correct for these differences using a Procrustes analysis [13], followed by contrast stretching. The translation and rotation of images can create ‘borders’ where clipped images no longer fully overlap, therefore, we next crop outer edges.

Once the images are maximally aligned, we generate a pixel-by-pixel difference map. Small inconsistencies are common between these images. In addition to physical differences (e.g. dust coverage), image variations frequently derive from time-dependent photographic conditions such as lighting. We consider only pixels with value differences above a tuned threshold. The resulting product from this filter is a binary map indicating points that exceed a tuned threshold value and could be potential impact craters.

We then identify groups of contiguous pixels in each difference map, discarding single-pixel groups. These correspond to a number of features in addition to fresh craters that must be separated from potential impact sites. These include both lighting artifacts as well as non-impact-related sedimentary processes such as wind streaks. As a first pass, we exclude all pixel groups with an area small enough to prevent high-confidence geological interpretations at the ~6 m/px CTX resolutions; this also serves to eliminate noise in the difference map. In order to isolate likely impact candidates, we calculate each region’s circularity- perimeter/area ratio, eccentricity, and convexity, and compare these with values from known impacts [9]. Regions with reasonable parameters for potential craters are flagged (Fig. 1C). The parameters are tuned to minimize false negatives, resulting in a large number of false positives. The final step is human assessment, selecting likely impact features from among the extracted candidates.

Implications: The automated methods demonstrated in this work allow for a systematic search for fresh impacts at a scale and level of detail not achievable by humans alone. Application of this tool globally on Mars will likely yield a number of yet undiscovered recent impacts. These impacts, along with those already identified [9], constitute the best data for estimating a modern cratering rate and impact flux to Mars. Furthermore, the null detections from this tool can be incorporated into a statistically rigorous estimate of impact flux that accounts for the non-uniform sampling of the planet. Tests for longitudinal and elevation dependence can also be achieved, but all these require the statistical rigor and global reach and high resolution made possible with this tool.

References: [1] Bourke M. C. et al. (2008) *Geomorphology, 94(1-2),* 247-255. [2] Pilorget C. and Forget F. (2016) *Nature Geoscience, 9(1),* 65-69. [3] Malin M. C. et al. (2006) *Science, 314(5805),* 1573–1577. [4] Hartmann, W. K., & Neukum, G. (2001). *Chronology and evolution of Mars* (165-194). Springer, Dordrecht. [5] Barlow, N. G., & Perez, C. B. (2003). *JGR: Planets*, 108(E8). [6] Holo, S. J., Kite, E. S., & Robbins, S. J. (2018). *EAPS Letters*, 496, 206-214. [7] Quantin, C. et al. (2007). *Icarus*, 186(1), 1-10. [8] Malin, M. C. et al. (2006). *Science*, 314(5805), 1573-1577. [9] Daubar, I. J. et al. (2015,). In *LPSC* (Vol. 46, p. 2468). [10] Daubar, I. J. et al. (2013). *Icarus*, 225(1), 506-516. [11] Teanby, N and Wookey, J, (2011), *Physics of Earth and Planetary Interiors*, 186(1-2), 70-80. [12] Malin, M. C et al. (2007). *JGR: Planets*, 112(E5). [13] Gower, J. C. (1975). *Psychometrika*, 40(1), 33-51.